Chapter 8

Shape — case studies

8.1 Introduction and synopsis

This chapter, like Chapter 6, is a collection of case studies. They illustrate the use of material indices which include shape. Remember: they are only necessary for the restricted class of problems in which section shape directly influences performance, that is, when the prime function of a component is to carry loads which cause it to bend, twist or buckle. And even then they are needed only when the shape is itself a variable, that is, when different materials come in different shapes. When all candidate-materials can be made to the *same* shapes, the indices reduce to those of Chapter 6.

Indices which include shape provide a tool for optimizing the co-selection of material-and-shape. The important ones are summarized in Table 8.1. Many were derived in Chapter 7; the others are derived here. Minimizing cost instead of weight is achieved by replacing density ρ by $C_m\rho$, where C_m is the cost per kilogram.

The selection procedure is, first, to identify candidate-materials and the section shapes in which each is available, or could be made. The relevant material properties* and shape factors for each are tabulated. The best material-and-shape combination is that with the greatest value of the appropriate index. The same information can be plotted onto Materials Selection Charts, allowing a graphical solution to the problem — one which often suggests further possibilities.

The method has other uses. It gives insight into the way in which natural materials — many of which are very efficient — have evolved. Bamboo is an example: it has both internal or microscopic shape and a tubular, macroscopic shape, giving it very attractive properties. This and other aspects are brought out in the case studies which now follow.

8.2 Spars for man-powered planes

Most engineering design is a difficult compromise: it must meet, as best it can, the conflicting demands of multiple objectives and constraints. But in designing a spar for a man-powered plane the objective is simple: the spar must be as light as possible, and still be stiff enough to maintain the aerodynamic efficiency of the wings (Table 8.2). Strength, safety, even cost, hardly matter when records are to be broken. The plane (Figure 8.1) has two main spars: the transverse spar supporting the wings, and the longitudinal spar carrying the tail assembly. Both are loaded primarily in bending (torsion cannot, in reality, be neglected, although we shall do so here).

Some 60 man-powered planes have flown successfully. Planes of the first generation were built of balsa wood and spruce. The second generation relied on aluminium tubing for the load-bearing

* The material properties used in this chapter are taken from the *CMS* compilation published by Granta Design, Trumpington Mews, 40B High Street, Trumpington CB2 2LS, UK.

Table 8.1 Examples of indices which include shape

(a) Stiffness and strength-limited design at minimum weight (or cost*)

Component shape, loading and constraints	*Stiffness-limited design*	*Strength-limited design*
Tie (tensile member) Load, stiffness and length specified, section-area free	$\frac{E}{\rho}$	$\frac{\sigma_f}{\rho}$
Beam (loaded in bending) Loaded externally or by self weight, stiffness, strength and length specified, section area free	$\frac{(\phi_B^e E)^{1/2}}{\rho}$	$\frac{(\phi_B^f \sigma_f)^{2/3}}{\rho}$
Torsion bar or **tube** Loaded externally , stiffness, strength and length specified, section area free	$\frac{(\phi_T^e E)^{1/2}}{\rho}$	$\frac{(\phi_T^f \sigma_f)^{2/3}}{\rho}$
Column (compression strut) Collapse load by buckling or plastic crushing and length specified, section area free	$\frac{(\phi_B^e E)^{1/2}}{\rho}$	$\frac{\sigma_f}{\rho}$

*For cost, replace ρ by $C_m\rho$ in the indices.

(a) Springs, specified energy storage at minimum volume or weight (or cost*)

Component shape, loading and constraints	*Flexural springs*	*Torsion springs*
Spring Specified energy storage, volume to be minimized	$\frac{(\phi_B^f \sigma_f)^2}{\phi_B^e E}$	$\frac{(\phi_T^f \sigma_f)^2}{\phi_T^e E}$
Spring Specified energy storage, mass to be minimized	$\frac{(\phi_B^f \sigma_f)^2}{\phi_B^e E\rho}$	$\frac{(\phi_T^f \sigma_f)^2}{\phi_T^e E\rho}$

*For cost, replace ρ by $C_m\rho$ in the indices.

Table 8.2 Design requirements for wing spars

Function	Wing spar
Objective	Minimum mass
Constraints	(a) Specified stiffness (b) Length specified

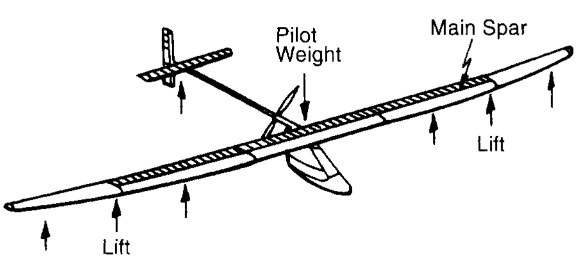

Fig. 8.1 The loading on a man-powered plane is carried by two spars, one spanning the wings and the other linking the wings to the tail. Both are designed for stiffness at minimum weight.

structure. The present, third, generation uses carbon-fibre/epoxy spars, moulded to appropriate shapes. How has this evolution come about? And how much further can it go?

The model and the selection

We seek a material-and-shape combination that minimizes weight for a given bending stiffness. The index to be maximized, read from Table 8.1, is

$$M_1 = \frac{(\phi_B^e E)^{1/2}}{\rho} \qquad (8.1)$$

Data for four materials are assembled in Table 8.3. If all have the same shape, M_1 reduces to the familiar $E^{1/2}/\rho$ and the ranking is that of the second last column. Balsa and spruce are significantly better than the competition. Woods are extraordinarily efficient. That is why model aircraft builders use them now and the builders of real aircraft relied so heavily on them in the past.

The effect of shaping the section, to a rectangle for the woods, to a box-section for aluminium and CFRP, gives the results in the last column. (The shape factors listed here are typical of commercially available sections, and are well below the maximum for each material.) Aluminium is now marginally better than the woods; CFRP is best of all.

The same information is shown graphically in Figure 8.2, using the method of Chapter 7. Each shape is treated as a new material with modulus $E^* = E/\phi_B^e$ and $\rho^* = \rho/\phi_B^e$. The values of E^* and ρ^* are plotted on the chart. The superiority of both the aluminium tubing with $\phi = 20$ and the CFRP box-sections with $\phi = 10$ are clearly demonstrated.

Postscript

Why is wood so good? With no shape it does as well or better than heavily-shaped steel. It is because wood *is* shaped: its cellular structure gives it internal shape (see p. 182), increasing the performance of the material in bending; it is nature's answer to the I-beam. Bamboo, uniquely, combines microscopic and macroscoptic shape (see next section).

But the technology of drawing thin-walled aluminium tubes has improved. Aluminium itself is stiffer than balsa or spruce, but it is also nearly 10 times denser, and that makes it, as a solid, far less attractive. As a tube, though, it can be given a shape factor which cannot be reproduced in wood. An aluminium tube with a shape factor $\phi_B^e = r/t = 20$ is as good as solid balsa or spruce; one with a thinner wall is better — a fact that did not escape the designers of the second generation of man-powered planes. There is a limit, of course: tubes that are too thin will kink (a local elastic buckling); as shown in Chapter 7, this sets an upper limit to the shape factor for aluminium at about 40.

Table 8.3 Materials for wing spars

Material	*Modulus E (GPa)*	*Density ρ (Mg/m³)*	*Shape factor* ϕ_B^e	*Index* $E^{1/2}/\rho$	*Index* M_1^* $((GPa)^{1/2}/Mg/m^3)$
Balsa	4.2–5.2	0.17–0.24	1–2	**11**	11–15
Spruce	9.8–11.9	0.36–0.44	1–2	9	9–12
Steel	200–210	7.82–7.84	25–30	1.8	9–10
Al 7075 T6	71–73	2.8–2.82	15–25	3	12–15
CFRP	100–160	1.5–1.6	10–15	7	**23–28**

*The range of values of the indices are based on means of the material properties and corresponds to the range of values of ϕ_B^e.

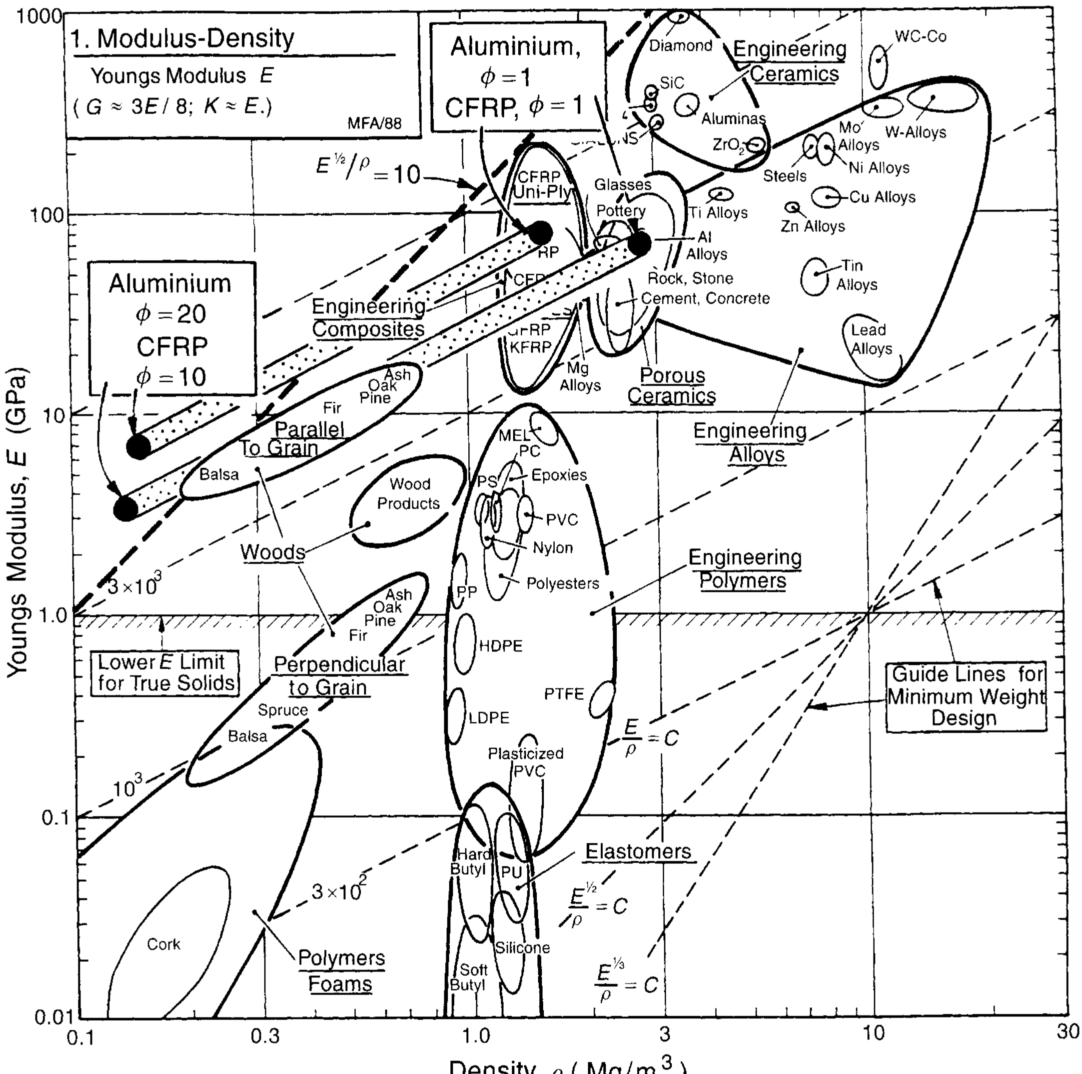

Fig. 8.2 The materials-and-shapes for wing-spars, plotted on the modulus–density chart. A spar made of CFRP with a shape factor of 10 outperforms spars made of aluminium ($\phi = 20$) and wood ($\phi \approx 1$).

The last 20 years has seen further development: carbon-fibre technology has reached the market place. As a solid beam, carbon-fibre reinforced polymer laminates are nearly as efficient as spruce. Add a bit of shape (Table 8.3) and they are better than any of the competing materials. Contemporary composite technology allows shape factors of at least 10, and that gives an increase in performance that — despite the cost — is attractive to plane builders.

Further reading: man-powered flight

Drela, M. and Langford, J.D. (1985) Man-powered flight, *Scientific American*, January issue, p. 122.

Related case studies

Case Study 8.3: Forks for a racing bicycle
Case Study 8.4: Floor joists

8.3 Forks for a racing bicycle

The first consideration in bicycle design (Figure 8.3) is strength. Stiffness matters, of course, but the initial design criterion is that the frame and forks should not yield or fracture in normal use. The loading on the forks is predominantly *bending*. If the bicycle is for racing, then the mass is a primary consideration: the forks should be as light as possible. What is the best choice of material and shape? Table 8.4 lists the design requirements.

The model and the selection

We model the forks as beams of length ℓ which must carry a maximum load P (both fixed by the design) without plastic collapse or fracture. The forks are tubular, of radius r and fixed wall-thickness t. The mass is to be minimized. The fork is a light, strong beam. Further details of load and geometry are unnecessary: the best material and shape, read from Table 8.1, is that with the

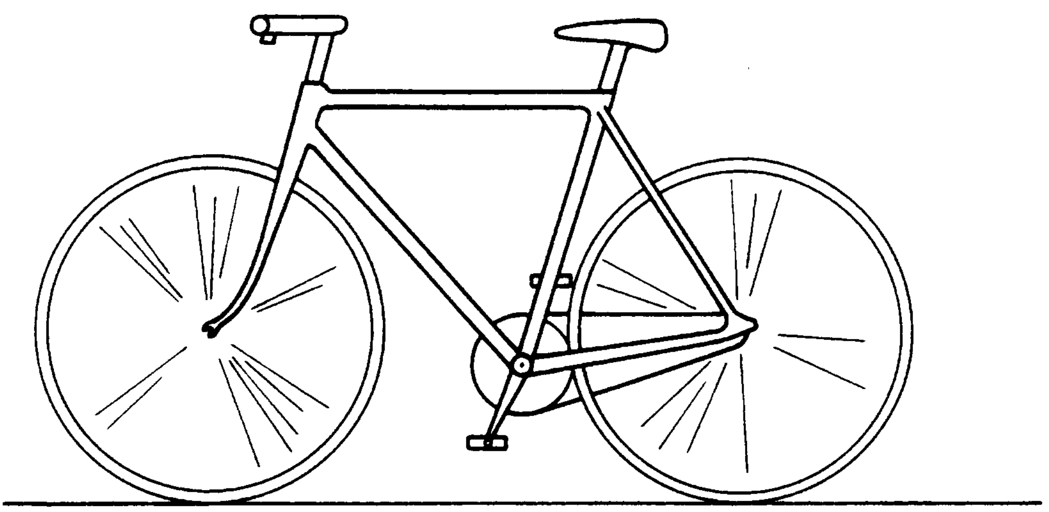

Fig. 8.3 The bicycle. The forks are loaded in bending. The lightest forks which will not collapse plastically under a specified design load are those made of the material and shape with the greatest value of $(\phi_B^f \sigma_f)^{2/3}/\rho$.

Table 8.4 Design requirements for bicycle forks

Function	Bicycle forks
Objective	Minimize mass
Constraints	(a) Must not fail under design loads — a strength constraint (b) Length specified

Table 8.5 Material for bicycle forks

Material	*Strength σ_f (MPa)*	*Density ρ (Mg/m^3)*	*Shape factor ϕ_B^f*	*Index $\sigma_f^{2/3}/\rho$*	*Index M_3^* ((MPa)$^{2/3}$/Mg/m^3)*
Spruce (Norwegian)	70–80	0.46–0.56	1–1.5	**36**	36–50
Bamboo	80–160	0.6–0.8	2.4–2.8	(33)	59–65
Steel (Reynolds 531)	770–990	7.82–7.83	7–8	12	44–48
Alu (6061–T6)	240–260	2.69–2.71	5.5–6.3	15	47–51
Titanium 6-4	930–980	4.42–4.43	5.5–6.3	22	69–75
Magnesium AZ 91	160–170	1.80–1.81	4–4.5	17	42–46
CFRP	300–450	1.5–1.6	4–4.5	33	**83–90**

*The range of values of the indices are based on means of the material properties and corresponds to the range of values of ϕ_B^e.

greatest value of

$$M_3 = \frac{(\phi_B^f \sigma_f)^{2/3}}{\rho} \tag{8.2}$$

Table 8.5 lists seven candidate materials. Solid spruce or bamboo are remarkably efficient; without shape (second last column) they are better than any of the others. Bamboo is special because it grows as a hollow tube with a macroscopic shape factor ϕ_B^f between 3 and 5, giving it a bending strength which is much higher than solid spruce (last column). When shape is added to the other materials, however, the ranking changes. The shape factors listed in the table are achievable using normal production methods. Steel is good; CFRP is better; Titanium 6-4 is better still. In strength-limited applications magnesium is poor despite its low density.

Postscript

Bicycles have been made of all seven of the materials listed in the table — you can still buy bicycles made of six of them (the magnesium bicycle was discontinued in 1997). Early bicycles were made of wood; present-day racing bicycles of steel, aluminium or CFRP, sometimes interleaving the carbon fibres with layers of glass or Kevlar to improve the fracture-resistance. Mountain bicycles, for which strength and impact resistance are particularly important, have steel or titanium forks.

The reader may be perturbed by the cavalier manner in which theory for a straight beam with an end load acting normal to it is applied to a curved beam loaded at an acute angle. No alarm is necessary. When (as explained in Chapter 5) the variables describing the functional requirements (F), the geometry (G) and the materials (M) in the performance equation are separable, the details of loading and geometry affect the terms F and G but not M. This is an example: beam curvature and angle of application of load do not change the material index, which depends only on the design requirement of strength in bending at minimum weight.

Further reading: bicycle design

Sharp, A. (1993) *Bicycles and Tricycles, an Elementary Treatise on their Design and Construction*, The MIT Press, Cambridge, MA.
Watson, R. and Gray, M. (1978) *The Penguin Book of the Bicycle*, Penguin Books, Harmondsworth.
Whitt, F.R. and Wilson, D.G. (1985) *Bicycling Science*, 2nd edition, The MIT Press, Cambridge, MA.
Wilson, D.G. (1986) A short history of human powered vehicles, *The American Scientist*, **74**, 350.

Related case studies

Case Study 8.2: Wing spars for man powered planes
Case Study 8.4: Floor joists: wood or steel?

8.4 Floor joists: wood or steel?

Floors are supported on *joists:* beams which span the space between the walls. Let us suppose that a joist is required to support a specified bending load (the 'floor loading') without sagging excessively or failing; and it must be cheap. Traditionally, joists are made of wood with a rectangular section of aspect ratio 2:1, giving an elastic shape factor (Table 7.2) of $\phi_B^e = 2.1$. But steel, shaped to an I-section, could be used instead (Figure 8.5). Standard steel I-section joists have shape factors in the range $15 \leq \phi_B^e \leq 25$ (special I- sections can have much larger values). Are steel I-joists a better choice than wooden ones? Table 8.6 summarizes the design requirements.

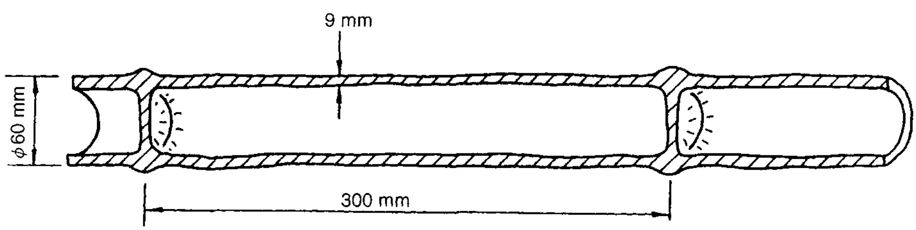

Fig. 8.4 The cross-section of a typical bamboo cane. The tubular shape shown here gives 'natural' shape factors of $\phi_B^e = 3.3$ and $\phi_B^f = 2.6$. Because of this (and good torsional shape factors also) it is widely used for oars, masts, scaffolding and construction. Several bamboo bicycles have been marketed.

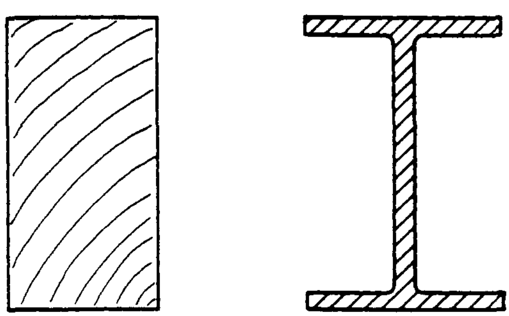

Fig. 8.5 The cross-sections of a wooden beam ($\phi_B^e = 2$) and a steel I-beam ($\phi_B^e = 10$). The values of ϕ are calculated from the ratios of dimensions of each beam, using the formulae of Table 7.2.

Table 8.6 Design requirements for floor joists

Function	Floor joist
Objective	Minimum material cost
Constraints	(a) Length specified (b) Minimum stiffness specified (c) Minimum strength specified

The model and the selection

Consider stiffness first. The cheapest beam, for a given stiffness, is that with the largest value of the index (read from Table 8.1 with ρ replaced by $C_m\rho$ to minimize cost):

$$M_1 = \frac{(\phi_B^e E)^{1/2}}{C_m\rho} \tag{8.3}$$

Data for the modulus E, the density ρ, the material cost C_m and the shape factor ϕ_B^e are listed in Table 8.7, together with the values of the index M_1 with and without shape. The steel beam with $\phi_B^e = 25$ has a slightly larger value M_1 than wood, meaning that it is a little cheaper for the same stiffness.

But what about strength? The best choice for a light beam of specified strength is that which maximizes the material index:

$$M_2 = \frac{(\phi_B^f \sigma_f)^{2/3}}{C_m\rho} \tag{8.4}$$

The quantities of failure strength σ_f, shape factor ϕ_B^f and index M_3 are also given in the table. Wood performs better than even the most efficient steel I-beam.

As explained in Chapter 7, a material with a modulus E and cost per unit volume $C_m\rho$, when shaped, behaves in bending like a material with modulus $E^* = E/\phi_B^e$ and cost $(C_m\rho)^* = C_m\rho/\phi_B^e$. Figure 8.6 shows the E–$C_m\rho$ chart with data for the wooden joists and the steel I-beams plotted onto it. The heavy broken line shows the material index $M_1 = (\phi_B^e E)^{1/2}/C_m\rho$, positioned to leave a small subset of materials above it. Woods with a solid circular section ($\phi_B^e = 1$) lie comfortably above the line; solid steel lies far below it. Introducing the shape factors moves the wood slightly (the shift is not shown) but moves the steel a lot, putting it in a position where it performs as well as wood.

Strength is compared in a similar way in Figure 8.7. It shows the $\sigma_f - C_m\rho$ chart. The heavy broken line, this time, is the index $M_3 = (\phi_B^f \sigma_f)^{2/3}/C_m\rho$, again positioned just below wood. Introducing shape shifts the steel as shown, and this time it does not do so well: even with the largest shape factor ($\phi_B^f = 10$) steel performs less well than wood. Both conclusions are exactly the same as those of Table 8.7.

Table 8.7 Materials for floor joists

Property	*Wood (pine)*	*Steel (standard)*
Density (Mg/m^3)	0.52–0.64	7.9–7.91
Flexural modulus (GPa)	9.8–11.9	208–212
Failure strength — MOR (MPa)	56–70	350–360
Material cost (\$/kg)	0.8–1.0	0.6–0.7
ϕ_B^e	2.0–2.2	15–25
ϕ_B^f	1.6–1.8	5.5–7.1
$E^{1/2}/C_m\rho$ $(GPa)^{1/2}/(k\$/m^3)^*$	6.3	2.8
$\sigma_f^{2/3}/C_m\rho$ $(MPa)^{2/3}/(k\$/m^3)^*$	30	9.7
M_1 $(GPa)^{1/2}/(k\$/m^3)^*$	8.9–9.3	10.8–14.0
M_2 $(MPa)^{2/3}/(k\$/m^3)^*$	41–44	30–36

*The range of values of the indices are based on means of the material properties and corresponds to the range of values of ϕ_B^e.

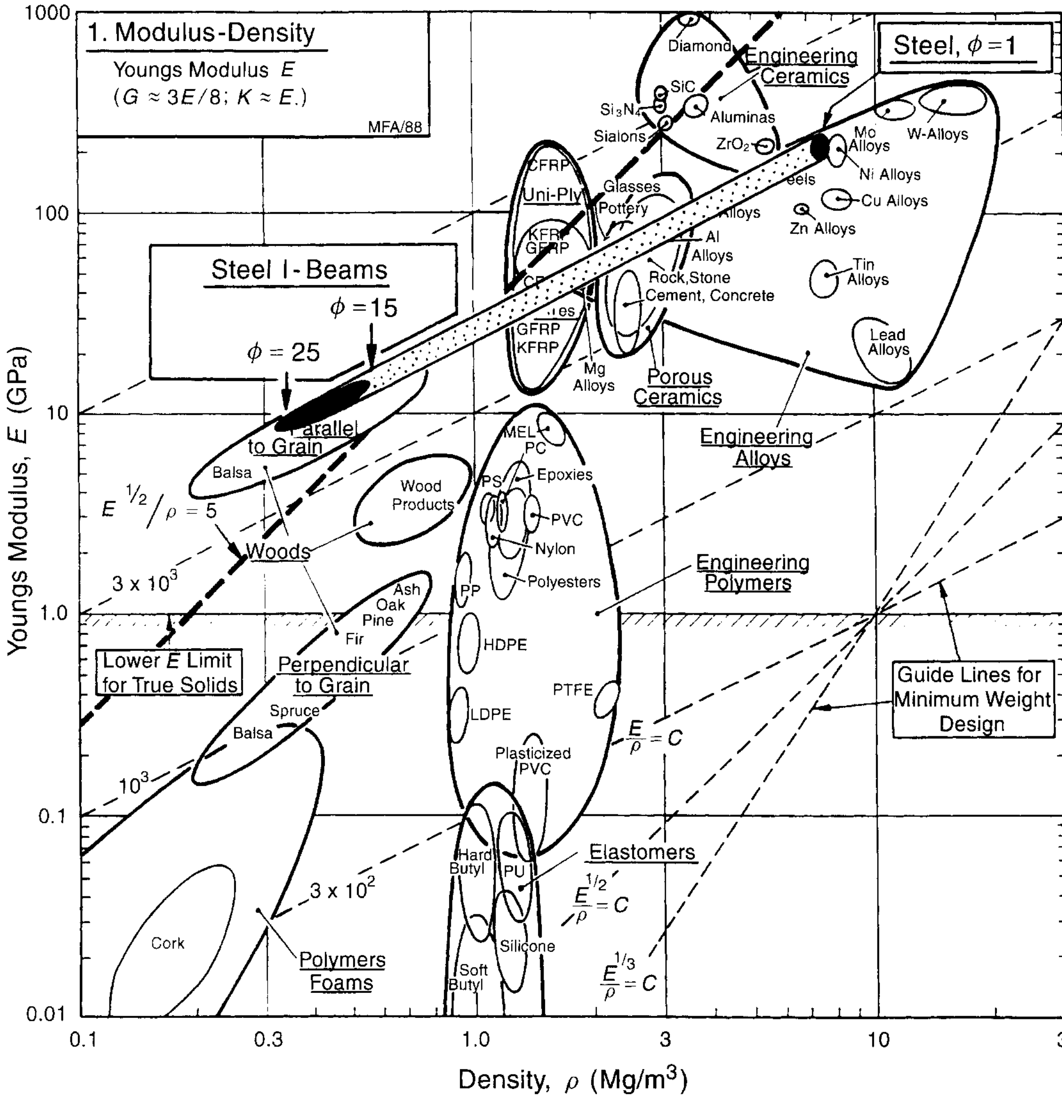

Fig. 8.6 A comparison of light, stiff beams. The heavy broken line shows the material index $M_1 = 5\,(\text{GPa})^{1/2}/(\text{Mg/m}^3)$. Steel I-beams are slightly more efficient than wooden joists.

Postscript

So the conclusion: as far as performance per unit material-cost is concerned, there is not much to choose between the standard wood and the standard steel sections used for joists. As a general statement, this is no surprise — if one were much better than the other, the other would no longer exist. But — looking a little deeper — wood dominates certain market sectors, steel dominates others. Why?

Wood is indigenous to some countries, and grows locally; steel has to come further, with associated transport costs. Assembling wood structures is easier than those of steel; it is more forgiving

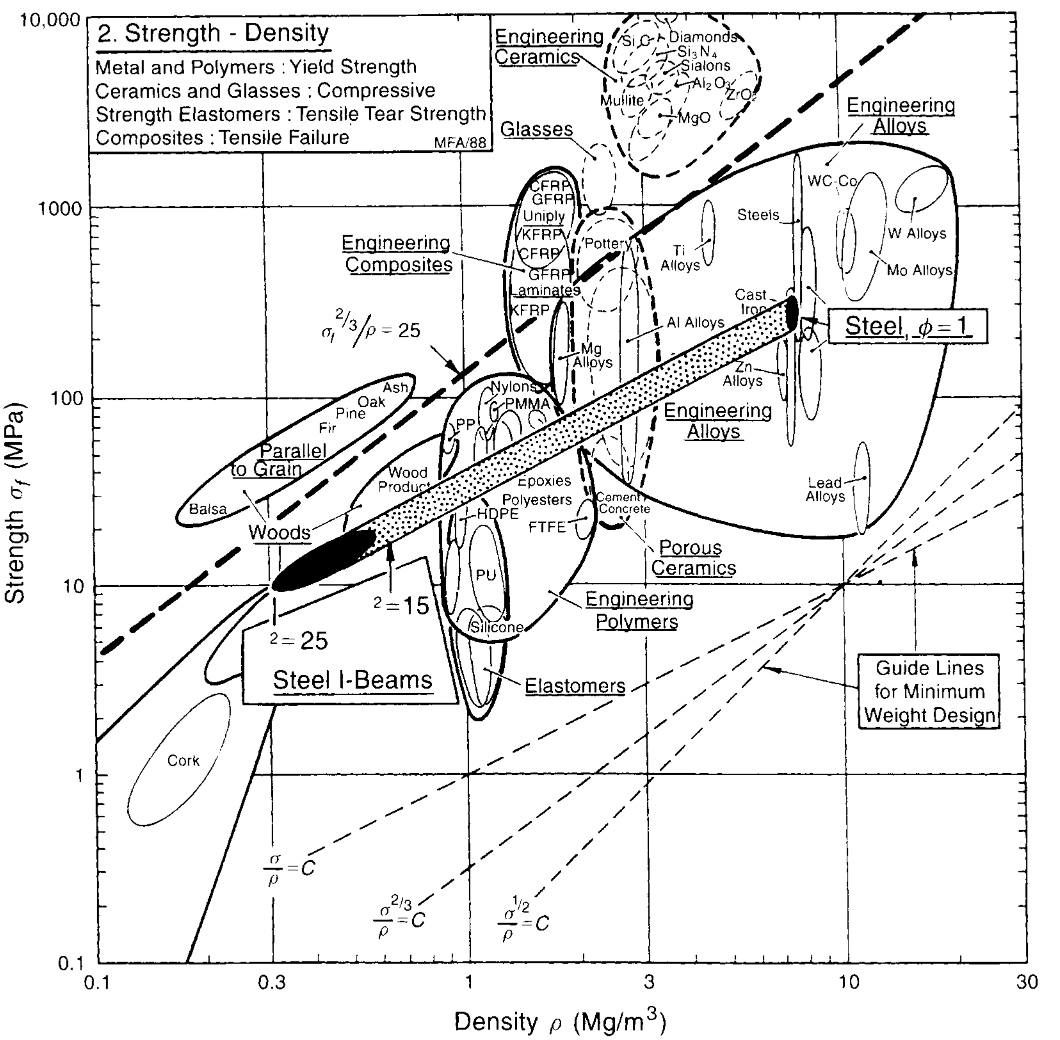

Fig. 8.7 A comparison of light, strong beams. The heavy broken line shows the material index $M_2 = 25\,(\mathrm{MPa})^{2/3}/(\mathrm{Mg/m^3})$. Steel I-beams are less efficient than wooden joists.

of mismatches of dimensions, it can be trimmed on site, you can hammer nails into it anywhere. It is a user-friendly material.

But wood is a variable material, and, like us, is vulnerable to the ravishes of time, prey to savage fungi, insects and small mammals. The problems so created in a small building — family home, say — are easily overcome, but in a large commercial building — an office block, for instance — they create greater risks, and are harder to fix. Here, steel wins.

Further reading

Cowan, H.J. and Smith, P.R. (1988) *The Science and Technology of Building Materials*, Van Nostrand Reinhold, New York.

Related case studies

Case Study 8.2: Spars for man-powered planes
Case Study 8.3: Forks for a racing bicycle

8.5 Increasing the stiffness of steel sheet

How could you make steel sheet stiffer? There are many reasons you might wish to do so. The most obvious: to enable stiffness-limited sheet structures to be lighter than they are now; to allow panels to carry larger compressive loads without buckling; and to raise the natural vibration frequencies of sheet structures. Bending stiffness is proportional to EI (E is Young's modulus, I is the second moment of area of the sheet, equal to $t^3/12$ per unit width). There is nothing much you can do to change the modulus of steel, which is always close to 210 GPa. But you can add a bit of shape. So consider the design brief of Table 8.8.

The model

The age-old way to make sheet steel stiffer is to corrugate it, giving it a roughly sinusoidal profile. The corrugations increase the second moment of area of the sheet about an axis normal to the corrugations themselves. The resistance to bending in one direction is thereby increased, but in the cross-direction it is not changed at all.

Corrugations are the clue, but — to be useful — they must stiffen the sheet in all directions, not just one. A hexagonal grid of dimple (Figure 8.8) achieves this. There is now no direction of bending that is not dimpled. The dimples need not be hexagons; any pattern arranged in such a way that you cannot draw a straight line across it without intersecting dimples will do. But hexagons are probably about the best.

Dimples improve all the section-properties of a sheet, in a way that can be estimated as follows. Consider an idealized cross-section as in the lower part of Figure 8.8, which shows the section A–A, enlarged. As before, we define the shape factor as the ratio of the stiffness of the dimpled sheet to that of the flat sheet from which it originated. The second moment of area of the flat sheet is

$$I_o = \frac{t^3}{12}\lambda \qquad (8.5)$$

That of the dimpled sheet with amplitude a is

$$I \approx \frac{1}{12}(2a + t)^2 \lambda t \qquad (8.6)$$

Table 8.8 Design requirements for stiffened steel sheet

Function	Steel sheet for stiffness-limited structures
Objective	Maximize bending stiffness of sheet
Constraints	(a) Profile limited to a maximum deviation ±5 times the sheet thickness from flatness (b) Cheap to manufacture

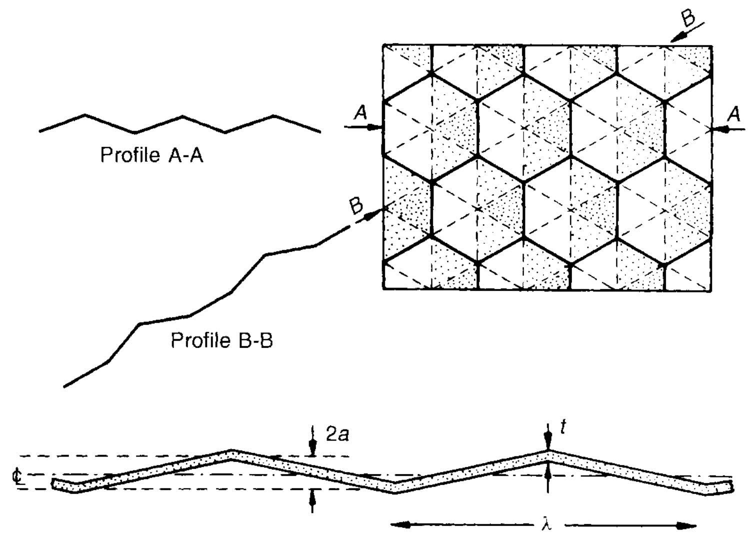

Fig. 8.8 A sheet with a profile of adjacent hexagonal dimples which increases its bending stiffness and strength. Shape factors for the section A–A are calculated in the text. Those along other trajectories are lower but still significantly greater than 1.

giving a shape factor, defined as before as the ratio of the stiffness of the sheet before and after corrugating (see the Appendix of Chapter 7):

$$\phi_B^e = \frac{I}{I_o} = \frac{(2a + t)^2}{t^2} \tag{8.7}$$

Note that the shape factor has the value unity when the amplitude is zero, but increases as the amplitude increases. The equivalent shape factor for failure in bending is

$$\phi_B^f = \frac{Z}{Z_o} = \frac{(2a + t)}{t} \tag{8.8}$$

These equations predict large gains in stiffness and strength. The reality is a little less rosy. This is because, while all cross-sections of the sheet are dimpled, only those which cut through the peaks of the dimples have an amplitude equal to the peak height (all others have less) and, even among these, only some have adjacent dimples; the section B–B, for example does not. Despite this, and limits set by the onset of local buckling, the gain is real.

Postscript

Dimpling can be applied to most rolled-sheet products. It is done by making the final roll-pass through mating rolls with meshing dimples, adding little to the cost. It is most commonly applied to sheet steel. Here it finds applications in the automobile industry including bumper armatures, seat frames, side impact bars: the material offers weight saving without loss of mechanical performance. Stiffening sheet also raises its natural vibration frequencies, making them harder to excite, thus helping to suppress vibration in panels.

But a final word of warning: stiffening the sheet may change its failure mechanism. Flat sheet yields when bent; dimpled sheet, if thin, could fail by a local buckling mode. It is this which ultimately limits the useful extent of dimpling.

Further reading

Fletcher, M. (1998) Cold-rolled dimples improve gauge strength, *Eureka*, May, p. 28.

8.6 Ultra-efficient springs

Springs, we deduced in Case Study 6.7, store energy. They are best made of a material with a high value of σ_f^2/E, or, if mass is more important than volume, then of $\sigma_f^2/\rho E$. Springs can be made more efficient still by shaping their section. Just how much more is revealed below.

We take as a measure of performance the energy stored per unit volume of solid of which the spring is made; we wish to maximize this energy. Energy per unit weight and per unit cost are maximized by similar procedures (Table 8.9).

The model

Consider a leaf spring first (Figure 8.9(a)). A leaf spring is an elastically bent beam. The energy stored in a bent beam, loaded by a force F, is

$$U = \frac{1}{2}\frac{F^2}{S_B} \tag{8.9}$$

where S_B, the bending stiffness of the spring, is given by equation (7.1), or, after replacing I by ϕ_B^e, by equation (7.25), which, repeated, is

$$S_B = \frac{C_1}{4\pi}\phi_B^e\frac{A^2}{\ell^3}E \tag{8.10}$$

Table 8.9 Design requirements for ultra-efficient springs

Function	Material-efficient spring
Objective	Maximum stored energy per unit volume (or mass, or cost)
Constraint	Must remain elastic under design loads

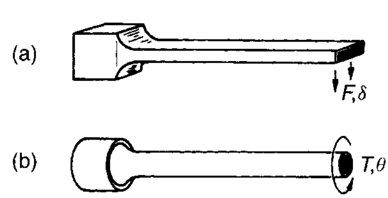

Fig. 8.9 Hollow springs use material more efficiently than solid springs. Best in bending is the hollow elliptical section; best in torsion is the tube.

The force F in equation (8.9) is limited by the onset of yield; its maximum value is

$$F_f = C_2 Z \frac{\sigma_f}{\ell} = \frac{C_2}{4\sqrt{\pi}\ell} \sigma_f \phi_B^f A^{3/2} \tag{8.11}$$

(The constants C_1 and C_2 are tabulated in Appendix A Section A3 and A4). Assembling these gives the maximum energy the spring can store:

$$\frac{U_{\max}}{V} = \frac{C_2^2}{8C_1} \left(\frac{(\phi_B^f \sigma_f)^2}{\phi_B^e E} \right) \tag{8.12}$$

where $V = A\ell$ is the volume of solid in the spring. The best material and shape for the spring — the one that uses the least material — is that with the greatest value of the quantity

$$\boxed{M_5 = \frac{(\phi_B^f \sigma_f)^2}{\phi_B^e E}} \tag{8.13}$$

For a fixed section shape, the ratio involving the two ϕs is a constant: then the best choice of material is that with the greatest value of σ_f^2/E — the same result as before. When shape is a variable, the most efficient shapes are those with large $(\phi_B^f)^2/\phi_B^e$. Values for these ratios are tabulated for common section shapes in Table 8.10; hollow elliptical sections are up to three times more efficient than solid shapes.

Torsion bars and helical springs are loaded in torsion (Figure 8.9(b)). The same calculation, but using equations (7.28) and (7.33), in the way that equations (8.10) and (8.11) were used, gives

$$\frac{U_{\max}}{V} = \frac{1}{16} \frac{(\phi_T^f \sigma_f)^2}{\phi_T^e G} \tag{8.14}$$

The most efficient material and shape for a torsional spring is that with the largest value of

$$\boxed{M_6 = \frac{(\phi_T^f \sigma_f)^2}{\phi_T^e E}} \tag{8.15}$$

(where G has been replaced by $3E/8$). The criteria are the same: when shape is not a variable, the best torsion-bar materials are those with high values of σ_f^2/E. Table 8.10 shows that the best shapes are hollow tubes, which have a ratio of $(\phi_T^f)^2/\phi_T^e$ which is twice that of a solid cylinder; all other shapes are less efficient. Springs which store the maximum energy per unit weight (instead of unit volume) are selected with indices given by replacing E by $E\rho$ in equations (8.13) and (8.15). For maximum energy per unit cost, replace $E\rho$ by $EC_m\rho$ where C_m is the cost per kg.

Postscript

Hollow springs are common in vibrating and oscillating devices and for instruments in which inertial forces must be minimized. The hollow elliptical section is widely used for springs loaded in bending; the hollow tube for those loaded in torsion. More about this problem can be found in the classic paper by Boiten.

Table 8.10 Shape factors for the efficiency of springs

Section shape	$(\phi_B^f)^2/\phi_B^e$	$(\phi_T^f)^2/\phi_T^e$
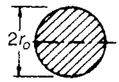	1	1
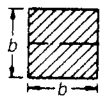	1.33	0.63
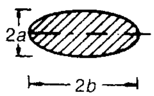	1	$\frac{(1+a^2/b^2)}{2}$ $(a<b)$
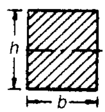	1.33	$\frac{2}{3}\left(1-0.6\left(\frac{b}{h}-\frac{b^2}{h^2}\right)\right)$ $(h>b)$
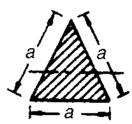	0.5	0.53
	2 $(t \ll r)$	2 $(t \ll r)$
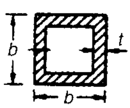	2.67 $(t \ll b)$	2
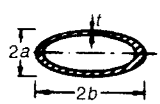	$\frac{1+3b/a}{1+b/a}$ $(a<b)$	$\frac{2b^3(1+a^2/b^2)}{(ab)^{3/2}(1+a/b)}$ $(a<b)$
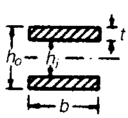	4	—
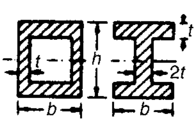	$\frac{4}{3}\frac{(1+3b/h)}{(1+b/h)}$	$\frac{2}{3}\frac{(1+4h/b)}{(1+h/b)}$
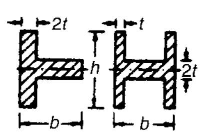	$\frac{3}{4}\frac{(1+4bt^2/h^3)}{(1+b/h)}$	$\frac{2}{3}\frac{(1+4b/h)}{(1+b/h)}$
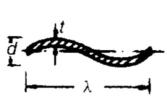	2	—

Further reading: design of efficient springs

Boiten, R.G. (1963) Mechanics of instrumentation, *Proc. I. Mech. E.*, **177**, p. 269.

Related case studies

Case Study 6.9: Materials for springs

8.7 Summary and conclusions

In designing components which are loaded such that they bend, twist or buckle, the designer has two groups of variables with which to optimize performance: the *material properties* and the *shape of the section*. The best choice of material depends on the shapes in which it is available, or to which it could potentially be formed. The procedure of Chapter 7 gives a method for optimizing the choice of material and shape.

Its use is illustrated in this chapter. Often the designer has available certain stock materials in certain shapes. Then that with the greatest value of the appropriate material index (of which a number were listed in Table 8.1) maximizes performance. Sometimes sections can be specially designed; then material properties and design loads determine a maximum practical value for the shape factor above which local buckling leads to failure; again, the procedure gives an optimal choice of material and shape. Further gains in efficiency are possible by combining microscopic with macroscopic shape.